The elastic behavior of zeolitic frameworks: the case of MFI type zeolite under high-pressure methanol intrusion.

Davide Comboni[a,b], Francesco Pagliaro[a], Paolo Lotti[a], G. Diego Gatta[a], Marco Merlini[a], Sula Milani[a], Massimo Migliori[c], Girolamo Giordano[c], Enrico Catizzone[d], Ines E. Collings[e], Michael Hanfland[e].

[a]Dipartimento di Scienze della Terra, Università degli Studi di Milano, Via Botticelli 23, 20133 Milano, Italy

[b]Dipartimento di Scienze della Terra e dell'Ambiente, Università degli Studi di Pavia, Via Adolfo Ferrata, 7, 27100 Pavia, Italy.

[c]Department of Environmental and Chemical Engineering, University of Calabria, via Bucci, 87036 Rende, Italy.

[d] ENEA-Italian National Agency for New Technologies, Energy and Sustainable Economic Development, Trisaia Research Centre, I-75026 Rotondella, Italy

[e]ESRF – European Synchrotron Radiation Facility, 71 Avenue des Martyrs, CS40220, 38043 Grenoble Cedex, France

*** Corresponding Author:** Davide Comboni, davide.comboni@unimi.it

Abstract

The high-pressure behavior of six synthetic zeolites with the MFI topology, characterized by different chemical composition (framework-Si partially replaced by Al or B and counterbalanced by Na or H as extra-framework cations), has been investigated by *in-situ* powder synchrotron X-ray diffraction using *silicone-oil* and *methanol* as hydrostatic pressure-transmitting fluids. For each sample, the compressibility in *silicone-oil* has been found to be considerably higher than that in *methanol*. This difference in terms of bulk elasticity is due to the adsorption of methanol already at P <0.1 GPa, with different magnitudes as a function of the sample crystal-chemistry. The high number of experimental pressure points allowed an accurate determination of the monoclinic-to-orthorhombic phase transition (MOPT), detected between 0.3 and 0.7 GPa in the samples compressed in *silicone-oil*, whereas the orthorhombic *Pnma* polymorph has been found to be stable already at ~ 0.1 GPa in four samples compressed in methanol. This suggests that the adsorption of methanol may increase the P-stability range of the orthorhombic *Pnma* phase. A comparative analysis of the effect of pressure on the methanol adsorption by MFI-zeolites with different chemical composition is provided, which offers potentially useful information on their application as catalysts in the methanol-to-olefins conversion processes.

Keywords: MFI-topology, Synchrotron X-ray diffraction, Pressure, Methanol Adsorption, Olefins, MOPT, in-situ characterization.

1. Introduction

Light olefins, such as ethylene, propylene and butene, are essential basic components for the petrochemical industry, and the industrial demand for these chemicals has been increasing every year. Olefins are widely used in industries as building blocks of polymers, plastics, membranes, rubbers, and also chemical intermediates [1]. Nowadays, 95% of the worldwide olefins production relies on the Steam Cracking (SC), which requires extensive energy consumption and produce large amounts of greenhouse gases as a result of the cracking of petroleum products [2]. Fluidized Catalytic Cracking (FCC) is one of the alternative synthesis routes which, using zeolites as reaction catalyst, allows milder conditions of synthesis. However, even though there are differences in terms of greenhouse gas emissions, energy consumption and costs, both SC and FCC make use of oil as raw material. Industrially, with the aim to improve olefins yield, the traditional catalyst for FCC unit (*i.e.*, USY equilibrium catalyst, E-cat) may be added with around 5-10%wt of ZSM-5 zeolite. Such a small amount of ZSM-5 is able to catalyze the conversion of gasoline-cut hydrocarbons towards LPG (and olefins) leading the LPG yield from 13.1% to 17.1% in Petrobras's FCC commercial unit [3]. ZSM-5-based catalyst is also used in refinery in dewaxing and isomerization unit, aiming to improve both fluidity and low temperature characteristics (*e.g.,* pour point). ExxonMobil Distillate Dewaxing (MDDW) and ExxonMobil Isomerization Dewaxing (MIDW) processes are commercial examples that use ZSM-5 as a catalyst [4]. On the other hand, ZSM-5 finds application as selective catalyst also in emerging technologies.

In this regard, because of the rising demand of both olefins and oil, alternative ways of production, such as the methanol to olefins (MTO) conversion, are particularly appealing. MTO process allows the conversion of methanol in light olefins, by using catalysts as the ZSM-5. Since methanol can be obtained from synthesis gas (a mixture of carbon monoxide and hydrogen), which is formed by steam reforming of natural gas or from the gasification of coal [5], the MTO process allows the production

of olefins bypassing oil as a raw precursor. Recently, the MTO process became promising and the first methanol to olefins plant was built in China in 2010, operating in the range of 460-480 °C and at atmospheric pressure [1,6–9].

Zeolites are microporous crystalline aluminosilicates with three-dimensional frameworks confining channels and cages with diameters similar to the molecular size of light olefins and aromatics. In the last decades, zeolites have been extensively employed in the oil and gas industries as catalysts in the cracking of hydrocarbons due to their unique key features, such as the efficient shape selectivity coupled to moderate synthesis costs and eco-friendliness [2,6,10,11]. The ZSM-5 belongs to the structure-type code Mobil Five (MFI) and are characterized by an Al-doped siliceous framework with the Si/Al ratio ranging from 10 to ∞; when this ratio exceeds 1000, the zeolite is known as "Silicalite-1" [12,13]. Indeed, MFI-type porous materials comprise of several synthetic phases, whereas the only mineral known with a MFI-framework topology is mutinaite [14]. The technological relevance of the MFI-type zeolite is due to its unique structure formed by $(Al,Si)O_4$ tetrahedra connected in such a way that a pore system, consisting of two intersecting channels, occurs within its zeolitic framework, as shown in Fig. 1. The channels, formed by 10-membered rings of $(Al,Si)O_4$ tetrahedra, have a diameter of ~ 5-6 Å and run parallel to the [010] direction (*i.e.*, *b*-crystallographic axis) whereas a non-linear pore path is observed along the [001] direction (*i.e.*, *c*-crystallographic axis).

ZSM-5 zeolites may crystallize in the $P2_12_12_1$ space group, though usually the *Pnma* and the $P2_1/n11$ space groups are far more common. In the literature, ZSM-5 crystals showing the last two space groups are generally referred to as "ORTHO" and "MONO", respectively [15–17]. A monoclinic-to-orthorhombic ($P2_1/n11$ → *Pnma*) phase transition (MOPT) has been reported in ZSM-5 zeolites [18]. The MOPT may be governed by different conditions such as the nature and concentration of the sorbate, temperature, pressure and the concentration of structural defects, and it is reported to be very sensitive to the chemical nature of the framework components [12,17,19–22]. For instance, the addition of a given fraction of aluminum (Si/Al less than 100) or of other trivalent dopants, such as iron and boron, in the tetrahedral framework is reported to lower the MOPT transition temperature

below the ambient conditions [23,24]. The pressure-induced MOPT, which can be detected in a powder diffraction experiment by a careful analysis of the Bragg peak splitting $133 - 13\bar{3}$, 451 - $45\bar{1}$, and 532 - $53\bar{2}$, was reported to take place between 1 and 1.5 GPa (at ambient temperature) and its reversibility is still matter of discussion [21,25,26]. Usually, at ambient conditions, only the surface of the zeolite crystallites is believed to be efficiently active in methanol-to-olefins conversion process. However, pressure can facilitate the methanol intrusion and diffusion through the zeolitic nanopores. This may bear a significant impact on the industrial applications of these zeolites as catalysts, as a *P*-mediated methanol intrusion into the zeolite cavities may pave the way for increasing the efficiency of the MTO conversion process.

This study is aimed to investigate, by means of *in situ* powder synchrotron X-ray diffraction, the *cold* (*i.e.*, at ambient-*T*) *P*-induced intrusion of methanol in different samples of synthetic MFI-zeolites, characterized by different framework and extra-framework compositions. The influence of the crystal chemistry of MFI-zeolites on the magnitude of *P*-mediated methanol intrusion, as well as the complex interplay between chemical composition, pressure and methanol loading on the occurrence of the MOPT phase transition, will be addressed and discussed. Since the zeolites grain size was found to play an important role on the magnitude of the *P*-induced intrusion phenomena [25-27], we have also investigated and compared the compressional behavior in methanol of a synthetic sample of Silicalite-1 by means of both *in-situ* powder and single-crystal synchrotron X-ray diffraction.

2. Experimental methods

2.1 Zeolite synthesis

Silicalite-1 and MFI-type zeolites containing different trivalent heteroatoms (*i.e.*, B, Fe and Al) were synthesised via hydrothermal crystallisation procedures already published. Al-containing MFI was synthesised by a slightly modifying procedure reported elsewhere [27], starting from this molar gel composition:

$$0.08\ Na_2O - 0.08\ TPABr - 0.005\ Al_2O_3 - 1\ SiO_2 - 20\ H_2O$$

Synthesis gel was prepared by dissolving, in a PP bottle, 1.97 g of NaOH (Aldrich), 0.316 g of sodium aluminate (54 wt% Al_2O_3, 54 wt% Na_2O, Aldrich) and 7.14 g of tetrapropyl ammonium bromide (TPABr, Aldrich), in 120.79 g of distilled water. Afterwards, 20.13 g of precipitated silica (Silica Gel 60, Merck) were added to the clear solution and the gel was stirred at room temperature for about 2 h. The gel was then transferred in a 200 ml stainless steel Teflon-lined autoclave and the crystallisation was performed in a static oven at 175 °C for 2 days.

Fe-containing MFI was synthesised by adopting the following molar gel composition [28]:

$$0.14\ Na_2O - 0.08\ TPABr - 0.005\ Fe_2O_3 - 1\ SiO_2 - 30\ H_2O$$

14.15 g of fumed silica (Aldrich) were added to an alkaline solution prepared by dissolving 2.64 g of NaOH (Aldrich) and 5.02 g of TPABr (Aldrich) in 42.30 g of distilled water. Afterwards, a second solution containing 0.68 g of H_3PO_4 (85%, Carlo Erba), 0.95 g of $Fe(NO_3)_3 \cdot 9H_2O$ (Aldrich) and 84.77 of distilled water was added to the alkaline solution. The resulting gel was stirred at room temperature for 1 h and then transferred in a 200 ml Teflon-lined stainless-steel autoclave and kept in a static oven at 175 °C for 2 days.

The following molar gel composition was used when synthesising the B-containing MFI [28]:

$$0.12\ Na_2O - 0.08\ TPABr - 0.017\ B_2O_3 - 1\ SiO_2 - 20\ H_2O$$

In this synthesis, 3 g of NaOH (Aldrich) and 6.98 g of TPABr (Aldrich) were dissolved in 78.68 g of distilled water. Afterwards, about 39.4 ml of 1M boric acid solution and 19.67 of precipitated silica were slowly added to the alkaline solution and the resulting gel was stirred at room temperature for 1 h. The crystallisation was carried out in a 200 ml Teflon-lined stainless-steel autoclave kept in a static oven at 175 °C for 2 days.

Silicalite-1 sample was synthesised starting from an alkaline gel with the following molar composition [29]:

$$0.08\ Na_2O - 0.08\ TPABr - 1\ SiO_2 - 20\ H_2O$$

The gel was prepared by adding 20.13 g of precipitated silica to an alkaline solution prepared by dissolving 2.14 g of NaOH and 7.14 g of TPABr in 120.8 g of distilled water. Similarly, to the other syntheses, the resulting gel was stirred at room temperature for 1 h and the crystallisation was carried out in a 200 ml Teflon-lined stainless-steel autoclave at 175 °C for 1 days.

For all the samples, after crystallisation, the zeolite powder was recovered by filtration and washed several times with distilled water and dried at 80 °C for 10 h. In order to remove the organic template, the solid was calcined at 550 °C in air flow with a heating rate of 10 °C/min. After calcination, both Al- and B-containing MFI samples were transformed in protonic form by ion exchange with ammonium solution followed by calcination as described elsewhere [30]. Chemical composition of the samples was measured by atomic absorption spectrometry (ContrAA®700 – Analytic Jena). The molar composition of the samples is reported in Table 1, as calculated from atomic absorption spectroscopy. For this analysis, a proper amount of sample was dissolved in hydrofluoric acid 40% Suprapur® (Sigma-Aldrich) and nitric acid 65% Suprapur® (Sigma-Aldrich) to completely dissolve the zeolite. Deionized water was used for dilution.

Larger Silicalite-1 crystals (50x20x20 μm^3 ca, Fig. 2) were synthesised according to an already developed procedure [31], by using the following synthesis gel composition:

$$0.02\ Na_2O - 0.08\ TPABr - 1\ SiO_2 - 10\ H_2O$$

The gel was prepared by dissolving at room temperature 0.43 g of NaOH (Sigma- Aldrich) and 5.7 g of TPABr (Merck) in 47.9 g of distilled water. Afterwards, 16 g of precipitated silica were slowly added to the clear solution and stirred at room temperature for 2 h. The obtained mixture was then transferred in a 90 ml Teflon-lined stainless-steel autoclave and kept in a static oven at 175 °C for 48 h. The obtained powder was recovered by vacuum filtration, washed several times with distilled water and dried at 80 °C for 10 h. To remove the organic template, the sample was calcined in a tubular quartz reactor under air flow at 550 °C for 8 h (heating rate 10 °C/min).

2.2 *High-pressure powder and single crystal synchrotron X-ray diffraction*

The H*P* synchrotron X-ray powder diffraction experiments were performed at the ID15B beamline of the European Synchrotron Radiation Facility (ESRF) in Grenoble, France. A stainless-steel foil (250 μm thick) was pre-indented to 70 μm and then drilled by spark-erosion, leading to a *P*-chamber ~250 μm in diameter. The experimental setup was the same for the twelve pressure ramps: the poly-crystalline samples were loaded in the *P*-chamber, along with some ruby spheres for pressure determination (pressure uncertainty ±0.05 GPa [32]), and a membrane-driven diamond anvil cell (DAC), with Boehler-Almax design anvils (culet diameter: 600 μm), has been used to generate hydrostatic pressure. Methanol and silicone oil were used as pressure-transmitting fluids. The adopted data collection strategy consisted, at any *P*-point, in a single-step ω-scan (-5°≤ ω ≤ +5°), with 10s of exposure time. The X-ray diffraction patterns were collected by a MAR555 flat-panel detector (at a distance of 400 mm from the sample position); 2θ-Intensity patterns have been integrated using the Fit2D software [33]. Rietveld full-profile fits have been performed using the GSAS package with the EXPGUI interface [34,35]. The pseudo-Voigt profile function by Thomson et al. [36] was used; the background curves were modelled with a Chebyshev polynomial with 20 to 31 coefficients. Scale factor, unit-cell parameters and zero-shift were allowed to vary for all the refinement cycles. The adopted structure models were those of monoclinic $P2_1/n$ and orthorhombic *Pnma* [37,38] H-ZSM zeolites, respectively: the atomic coordinates and displacement parameters were kept fixed for all the refinements. The refined unit-cell parameters as a function of pressure are reported in Fig. 3, Fig 3b and in Table S1, whereas the details pertaining to the Rietveld refinements are listed in Table S2. For the single-crystal H*P* experiment, the same experimental setup previously described was adopted, except for a sample-detector distance set to 270 mm. The data collection strategy consisted, at any *P*-point, in a step-wise ω-scan (-30°≤ ω ≤ +30°), with 1° step width and 1s exposure time per step. Indexing of the diffraction peaks and integration of their intensities (corrected for Lorentz-polarization effects) were performed using the CrysAlis package [39]. Corrections for absorption (caused by the DAC components) was applied using the semi-empirical *ABSPACK* routine

implemented in CrysAlis [39]. The refined unit-cell parameters as a function of pressure are reported in Fig. 4 and in Table S3. Further details pertaining to the beamline experimental setup are reported in Merlini and Hanfland [40].

3. Results and discussion

3.1 Chemical composition and space-group

Chemical data show that a high fraction of sodium is incorporated during the crystallisation, far in excess with respect to the theoretical amount needed to balance the negative charge induced by the Si substitution with tetrahedral trivalent heteroatoms. Even in the case of Silicalite-1, the sample that does not contain any trivalent framework cation, a significant fraction of sodium was detected (Table 1). Fegan et al. [41] reported that sodium may be incorporated in Silicalite-1 up to 4 atoms per unit cell, acting as stabilizer for silicate species during the crystallisation [31,42,43]. After ion exchange with ammonium solution, sodium was almost totally removed, whilst the fraction of aluminium or boron is preserved. The samples were named after their chemical differences, thus Na-SiO_2 (for Na-Silicalite-1), Na-Fe, Na-B, Na-Al, H-Al and H-B MFI. The lowest-*P* X-ray diffraction patterns collected for any sample (in *silicone oil*) showed that all of them crystallize in the $P2_1/n$ space group (hereafter referred as MONO, accordingly to the literature), except for the Na-B MFI (*Pnma*, hereafter ORTHO). The Na-Silicalite-1 single crystals (Fig. 2), in contrast to all the other samples, were found to crystallize in the $P2_12_12_1$ space group (already observed for MFI-zeolites by van Koningsveld et al. [16]), as deduced by the systematic extinctions of the X-ray diffraction pattern (Fig. 5).

3.2 Elastic behavior, phase transition and pressure-induced methanol adsorption

The description of the compressional behavior of the studied samples in the non-penetrating *silicone oil* provides a reference, which the compression in the penetrating *methanol* can be compared to, for a better characterization of the *P*-induced intrusion phenomena. In the literature, a change in the bulk compressibility of MFI at ~ 1 GPa has been commonly associated to the occurrence of the MOPT, as

deduced by the merging, in the orthorhombic polymorph, of several symmetry-independent Bragg peaks of the monoclinic structure, such as: 133 - $13\bar{3}$, 451- $45\bar{1}$, and 532 - $53\bar{2}$ (*e.g.*, Fig. 6) [21,25]. The MOPT has been investigated by several authors, who underlined its dependence to different variables, among those: temperature, pressure, the zeolite crystal chemistry, or the nature and concentration of the sorbate [12,17,44,18,19,21–26]. In this study, due to the relatively high number of experimental points at $P < 1$ GPa, we could accurately bracket the MOPT between 0.3(1) and 0.5(1) GPa in all but the Na-Fe MFI sample (in which the transition occurs between 0.40(5) and 0.70(5) GPa) and the Na-B MFI, for which an unambiguous split of the above-mentioned diagnostic peaks could not be detected, and the *Pnma* space group was, therefore, always assigned (*e.g.*, Fig. 6). These results agree with the observations of Haines et al. and Quartieri et al. [21,25], though providing a more accurate determination of the *P*-range at which the MOPT occurs, valid at least for the investigated zeolite compositions. As the deformation of the crystal structure is ultimately reflected by its elastic parameters (*e.g.*, its isothermal bulk modulus), the adsorption of methanol molecules in the zeolitic channels, as well as the modification of the symmetry of the crystal (*e.g.*, due to the MOPT), is expected to generate appreciable changes of the elastic parameters themselves. More in detail, the adsorption of methanol molecules should lead to higher $K_{P0,T0}$ with respect to the values obtained by compressing the zeolites in the non-penetrating *silicone-oil*. In order to describe the (isothermal) compressional behavior of the MFI-zeolites compressed respectively in *silicone-oil* and *methanol*, second-order Birch-Murnaghan Equations of State (BM2-EoS) [45] were fitted to the experimental *V*-*P* data, weighted by their uncertainties, using the EoS Fit 7.0 software [46], taking into account the different compressional regimes experienced by the samples, which will be described in detail later (Table 2). This isothermal EoS is based on the assumption that the high-pressure strain energy in a solid can be expressed as a Taylor series in the Eulerian finite strain, defined as $fe = [(V_0/V)^{2/3} - 1]/2$ (where V_0 is the volume at ambient pressure and temperature), and allows to obtain the isothermal bulk modulus ($K_{P0,T0} = V^{-1}(\partial P/\partial V)_{T0} = \beta^{-1}{}_{P0,T0}$, where $\beta_{P0,T0}$ is the volume

compressibility coefficient at room conditions) and its *P*-derivatives. Expansion in the Eulerian strain polynomial has the following form:

$$P(fe) = 3K_{P0,T0}\, fe\, (1 + 2fe)^{5/2}\, \{1 + 3/2(K' - 4)fe + 3/2[K_{P0,T0}K'' + (K'- 4)(K'-3) + 35/9]\, fe^2 + ...\},$$

where $K'=\partial K_{P0,T0}/\partial P$ and $K''=\partial^2 K_{P0,T0}/\partial P^2$

The refined intrinsic bulk moduli (compression in the non-penetrating *silicone oil*) in the lower *P*-range (up to ~ 0.6 GPa, thus before the MOPT, see Table 2), show that the investigated zeolites share the same elastic response, suggesting that, at least in the first compressional regime, the crystal chemical variations do not have an appreciable affect the bulk compressibility. However, in the *silicone oil* ramps, at $P >$ ~ 0.5 GPa (*i.e.,* above the occurrence of the MOPT pressure), a significant increase in the bulk compressibility is observed for all the zeolites (Table 2). This is also observed for the Na-B-MFI sample, for which the orthorhombic structure was assigned already in the lower *P*-regime, possibly suggesting that the absence of the peaks split, diagnostic of the monoclinic polymorph, may be induced by an experimental peak broadening (see Table 2). A second change in the compressional behavior is observed at ~ $P >$ 1 GPa, where a stiffening is experienced by all the samples. Unfortunately, Rietveld refinements of the structural parameters have been tried, but unsuccessfully. Therefore, if the first change of the compressional behavior can be reasonably assigned to the MOPT, the absence of structural information prevents a discussion on the second change. Overall, the refined bulk moduli, reported in Table 2, confirm the "extreme" compressibility of these zeolites, as already reported by Quartieri et al. [21,44] and Arletti et al. [47].

As can be observed in Fig. 3a and 3b, which show the *P*-*V* evolution of the studied MFI-zeolites, the elastic response of all the samples compressed in the penetrating *methanol* is drastically different than that in *silicone oil*. All the samples exhibit a significantly lower compressibility in methanol, suggesting a relevant intrusion of the fluid molecules into the zeolitic structural cavities, yet in the lower pressure range. The observed "stiffer" behavior is, therefore, a result of the "pillar effect" (*sensu* Gatta et al. [48,49]) played by the adsorbed extra-framework CH_3OH molecules, which hinder the *P*-

induced framework deformation. However, the magnitude of such intrusion appears different among the investigated samples. In order to better describe such differences, we plotted the $\Delta V\%$ *vs.* P of all the studied MFI-zeolites. $\Delta V\%$ is defined as:

$$\Delta V\% = 100 - \left(\frac{V_i}{V_0} \cdot 100\right)$$

where V_i and V_0 are, respectively, the i-th volume and the reference volume (*i.e.,* the first volume obtained in each ramp). At $P < 0.4$ GPa, Na-silicalite1 and Na-Fe MFI are apparently the less compressible samples, thus suggesting a potential higher magnitude of methanol intrusion (Fig. 7). However, at higher pressures, the (Na,H)-(Al,B)-MFI samples are clearly less compressible than the others, suggesting a potential crystal-chemical control on the magnitude of methanol intrusion in this P-range (Fig. 7). As the methanol adsorption is reasonably a progressive process, we cannot exclude that a second methanol adsorption phase, more pronounced in particular in (Na,H)-(Al,B)-MFI over Na-Silicalite-1 and Na-Fe MFI, takes place approximately at 0.8(1) GPa (*i.e.*, the cross-over pressure at which the $\Delta V\%$ of Na-Silicalite-1 and the Na-Fe MFI becomes higher than that of the other MFI-zeolites, see Fig.7)., Such a phenomenon could be reasonably due to the lower steric obstruction of the structural void, as in Na-Fe MFI, Fe^{3+} is concentrated in the T site of the TO_4 tetrahedra (shown in other studies, *e.g.,* [50]) and in Na-Silicalite-1 the zeolitic channels, due to the synthesis protocol, are also occupied only by H^+. It is worth to underline that, in the *methanol* ramps, no unambiguous split, in all but Na-Silicalite-1 and Na-Fe MFI, of the diagnostic peaks of the monoclinic polymorph was detected. Previous papers demonstrated that the MOPT is influenced also by the sorbate loading (*e.g.,* Haines et al. [25]), although it is interesting to note that, in this study, the pressure at which it occurs in Na-Silicalite-1 when compressed in *methanol* (between 0.46(5) and 0.57(5) GPa) corresponds, within the experimental uncertainty, with that observed in the *silicone oil* experiment (between 0.40(5) and 0.48(5) GPa). For the Na-Al, H-B and H-Al MFI samples compressed in *methanol* (*i.e.,* those MFI zeolites for which no unambiguous split of the diagnostic peaks was observed), the orthorhombic polymorph seems to be stable already at the lowest investigated pressure

conditions (0.02(5) GPa), suggesting a stabilizing role played by the intruded *methanol* molecules, which lowers the pressure at which the MOPT occurs down to (almost) ambient pressure. This confirms the critical control exerted by the extra-framework population on the high-pressure behavior of zeolites (*e.g.,* [51–55]). For all the MFI-zeolites, a data collection at ambient pressure was performed after decompression to verify the reversibility of the *methanol* adsorption. Interestingly, all the MFI-zeolites (but Na-B MFI, for which the powder was irremediable lost due to the fluid+sample dispersion from the DAC pressure chamber) were found to be monoclinic, as the diffraction patterns showed an unambiguous split of the 133 - $13\bar{3}$ reflection peaks (Tab. S1). This is consistent with data in *silicone-oil*, confirming that the *methanol* adsorption, induced by pressure, lowers the pressure at which the MOPT occurs. The unit-cell volumes, refined from the data collected in decompression, indicate that the bulk compression is almost fully recovered: only minimal differences in all MFI-zeolites but Na-Silicalite-1 were found. It is rather interesting that the unit-cell volume, measured in decompression at ambient pressure, of Na-Silicalite-1 is higher than that measured before the compression in *methanol*. This suggests that, for Na-Silicalite-1, not all the methanol molecules are released during decompression, *i.e.* a partial adsorption irreversibility occurs. It is also interesting to compare the compressional evolution in *methanol* of the polycrystalline sample of Na-Silicalite-1 with that of the $P2_12_12_1$ polymorph investigated by single-crystal XRD. The results, shown in Fig. 6, show that, up to the pressure at which the MOPT occurs, the two samples (*i.e.*, single crystal and powder) share the same compressibility within the experimental uncertainty, suggesting that no changes arise in the *methanol* adsorption process as a function of the crystal size. This behavior is in contrast with what shown, for instance, by SiO_2-ferrierite compressed in a methanol:ethanol:water mixture [54], where a lower compressibility was reported for the polycrystalline sample with respect to single crystal. It is worth to note that, in this study, pure *methanol* was used as pressure-transmitting medium, potentially enhancing the adsorption phenomena, accordingly with the experimental findings of Comboni et al. [51], if compared to mix of molecules. At pressures above the MOPT (*i.e.,* at $P \geq 0.57$ GPa), the *Pnma* polycrystalline sample

seems slightly more compressible than the single-crystal counterpart, which preserves the $P2_12_12_1$ space-group within the entire investigated *P*-range.

4. Concluding remarks

The comparative compressional behavior of different samples of MFI-zeolites, in the non-penetrating *silicone oil* and in the penetrating *methanol*, was studied to better characterize the pressure-induced *methanol*-zeolites interactions, even to explore the potential utilization of pressure as a physical variable able to promote the efficiency of these zeolites as catalysts in the MTO conversion process. The obtained results show that:

- All the MFI-zeolites of this study adsorb *methanol* under compression;
- At low pressure (< 0.4 GPa), the Na-Fe and the Na-Silicalite-1 are able to adsorb a higher number of methanol molecules per unit cell, as shown by their compressibility parameters;
- At higher pressure (> 0.8(1) GPa), the (Na,H)-(Al,B)-MFI samples are clearly less compressible than the others, suggesting a potential crystal-chemical control on the magnitude of *methanol* intrusion;
- When compressed in *silicone oil*, the $P2_1/n11$ → *Pnma* MOPT of all the MFI zeolites occurs between 0.3(1) and 0.7(1) GPa, as shown by the split of diagnostic reflection peaks (*e.g.*, $133, 13\bar{3}$);
- All the MFI-zeolites of this study, excluding the Na-Silicalite-1, show a perfectly reversible behavior upon decompression. In Na-Silicalite-1, the higher unit-cell volume measured at room conditions after decompression, with respect to the one measured before compression, suggests that not all the *P*-intruded *methanol* molecules are released during decompression; the *P*-mediated adsorption process appears to be (at least partially) irreversible.

Acknowledgments

ESRF is thanked for the allocation of beamtime and provision of synchrotron facilities at the ID15B beamline. DC, FP, PL, GDG, MM and SM acknowledge the support of the Italian Ministry of Education (MIUR) through the project “Dipartimenti di Eccellenza 2018-2022”

Table 1– Chemical composition of the investigated samples as determined by atomic absorption spectrometry before the transformation into the protonic form and the following calcination.

Sample	***Unit cell chemical composition***
Na-Al MFI	$Na_{2.51}Al_{0.81}Si_{95.19}O_{192}$
H-Al MFI	$Na_{0.05}Al_{0.87}Si_{95.13}O_{192}$
Na-B MFI	$Na_{2.84}B_{1.35}Si_{94.65}O_{192}$
H-B MFI	$Na_{0.02}B_{1.20}Si_{94.80}O_{192}$
Na-Fe MFI	$Na_{1.31}Fe_{0.89}Si_{95.11}O_{192}$
Na-Silicalite-1	$Na_{3.37}Si_{96}O_{192}$

Table 2. Refined elastic parameters pertaining to the different compressional regimes (*P*-range, GPa) of the investigated MFI zeolites compressed in *silicone oil* and *methanol*, based on isothermal II-BM Equation of State fits (*referred to single crystal data).

Sample	*P*-medium	*P*-range (GPa)	V_0 (Å^3)	K_0 (GPa)	K'	$\beta_{V,I}$ (GPa^{-1})
Na-Fe MFI	*Methanol*	0-0.71	5379(5)	50(5)	4	0.020(2)
Na-Fe MFI	*Methanol*	0.93-2.06	5466(22)	20(1)	4	0.050(3)
Na-Fe MFI	*S. oil*	0-0.44	5380(10)	21(4)	4	0.048(9)
Na-Fe MFI	*S. oil*	0.44 -1.06	5461(41)	11(2)	4	0.09(2)
Na-Fe MFI	*S. oil*	1.34-1.91	5333(50)	18(3)	4	0.056(9)
Na-Silicalite-1	*Methanol*	0-0.46	5365(3)	52(7)	4	0.019(3)
Na-Silicalite-1	*Methanol*	0.57-1.54	5416(13)	27(2)	4	0.037(3)
Na-Silicalite-1*	*Methanol*	0-0.65	5374(4)	50(6)	4	0.020(2)
Na-Silicalite-1*	*Methanol*	0.82-2.12	5503(24)	23(2)	4	0.043(4)
Na-Silicalite-1	*S. oil*	0-0.40	5382(12)	21(5)	4	0.05(1)
Na-Silicalite-1	*S. oil*	0.48-0.93	5425(48)	13(2)	4	0.08(1)
Na-Silicalite-1	*S. oil*	1.15-2.02	5249(22)	27(2)	4	0.037(3)
H-Al MFI	*Methanol*	0-0.41	5370(5)	33(5)	4	0.030(5)
H-Al MFI	*Methanol*	0.56-2.08	5399(6)	40(1)	4	0.025(1)
H-Al MFI	*S. oil*	0-0.29	5365(14)	14(4)	4	0.07(2)
H-Al MFI	*S. oil*	0.41-0.99	5358(32)	14(2)	4	0.07(1)
H-Al MFI	*S. oil*	1.12-2.03	5265(28)	21(2)	4	0.048(5)
Na-Al MFI	*Methanol*	0-0.95	5397(3)	51(3)	4	0.02(1)
Na-Al MFI	*Methanol*	1.10-2.04	5449(15)	37(3)	4	0.027(2)
Na-Al MFI	*S. oil*	0-0.52	5363(10)	21(8)	4	0.05(2)
Na-Al MFI	*S. oil*	0.52-1.08	5400(36)	14(2)	4	0.07(1)
Na-Al MFI	*S. oil*	1.41-2.16	5337(41)	19(2)	4	0.053(6)
H-B MFI	*Methanol*	0-0.50	5332(5)	35(4)	4	0.029(3)
H-B MFI	*Methanol*	1.14-2.25	5401(13)	34(2)	4	0.029(2)
H-B MFI	*S. oil*	0-0.35	5354(9)	22(4)	4	0.046(2)
H-B MFI	*S. oil*	0.52-1.23	5400(29)	14(1)	4	0.071(5)
H-B MFI	*S. oil*	1.35-2.18	5310(31)	20(2)	4	0.050(5)
Na-B MFI	*Methanol*	0-0.78	5388(8)	41(6)	4	0.024(4)
Na-B MFI	*Methanol*	1.10-1.98	5519(24)	25(2)	4	0.040(3)
Na-B MFI	*S. oil*	0-0.31	5364(11)	20(5)	4	0.05(1)
Na-B MFI	*S. oil*	0.40-1.00	5383(27)	14(2)	4	0.07(1)
Na-B MFI	*S. oil*	1.15-2.09	5204(15)	36(3)	4	0.028(2)

Fig. 1. Crystal structure of the MFI- framework viewed down [010], Si- atoms are shown in red, oxygen atoms in blue.

Fig. 2. SEM micrographs of the synthesized single crystals of Na-Silicalite-1.

Fig. 3. (a) High-pressure evolution of the normalized unit-cell volumes of the different MFI-zeolites, compressed in *methanol* (*black squares* for data collections in compression and *blue triangles* for data collections in decompression) and in *silicone-oil* (*red spheres*) [Na-Silicalite-1, *top left*; Na-Fe MFI, *top right*; Na-B MFI, *middle left*; H-Al MFI *middle right*; Na-Al MFI *bottom left*; H-B MFI, *bottom right*]. **(b)** Overall view of the methanol *(right side*) and *silicone-oil* ramps (*left side*) [Na-B MFI in *black squares*, H-B MFI in *red spheres*, Na-Al MFI in *blue upwards triangles*, H-Al MFI in *dark cyan downward triangles*, Na-Silicalite-1 in *pink leftward triangles* and Na-Fe MFI in *olive-green rightwards triangles*].

Fig. 4. High-pressure evolution of the normalized unit-cell volumes of the Na-Silicalite-1 samples (single crystal data in *black squares*, powder data before the MOPT in *red spheres*, powder data after the MOPT in *blue triangles*, green diamond represents the data collection performed in decompression).

Fig. 5. Reconstruction of the 0*kl** reciprocal lattice plane based on the experimental data. The presence of reflections (encircled in black dashed-line) violating the extinction condition 0*kl* ($k + l = 2n + 1$) suggests the $P2_12_12_1$ space group.

Fig. 6. Evolution of the133 and $13\bar{3}$ peaks in the XRD patterns of the H-B MFI sample compressed in *silicone oil* (monoclinic patterns in solid lines, first orthorhombic pattern in dash-dot line). The MOPT occurs between 0.35(5) and 0.52(5) GPa.

Fig. 7. Evolution of the ΔV% *vs*. *P*. Full symbols represent samples compressed in *methanol,* whereas empty symbols in *silicone-oil* (Na-B MFI in *black squares*, H-B MFI in *red spheres*, Na-Al MFI in *blue upwards triangles*, H-Al MFI in *green downward triangles*, Na-Silicalite-1 in *pink stars* and Na-Fe MFI in *orange diamonds*). At 0.8(1) GPa, the ΔV% of the Na-Silicalite-1 and Na-Fe MFI becomes higher than that of the other MFI-zeolites. Only data in compression are shown.

REFERENCES

[1] B.Y. Yu, I.L. Chien, Chem. Eng. Technol. 39 (2016) 2293–2303.

[2] S.M. Sadrameli, Fuel. 173 (2016) 285–297.

[3] L.A.S. Casali, S.D.F. Rocha, M.L.A. Passos, R. Bastiani, R.D.M. Pimenta, H.S. Cerqueira, Equilibrium FCC catalyst performance simulation based on mixtures of hydrothermal deactivated samples, in: M.. Ocelli (Ed.), Fluid Catal. Crack. VII Mater. Methods Process Innov., Elsevier, 2007: pp. 147–162.

[4] E.M. Flanigen, J.C. Jansen, H. van. Bekkum, Introduction to zeolite science and practice, Elsevier, 1991.

[5] M. Stocker, Microporous Mesoporous Mater. 29 (1999) 3–48.

[6] U. Olsbye, S. Svelle, M. Bjrgen, P. Beato, T.V.W. Janssens, F. Joensen, S. Bordiga, K.P. Lillerud, Angew. Chemie - Int. Ed. 51 (2012) 5810–5831.

[7] Z. Liu, J. Liang, Curr. Opin. Solid State Mater. Sci. 4 (1999) 80–84.

[8] Y. Qian, J. Liu, Z. Huang, A. Kraslawski, J. Cui, Y. Huang, Appl. Energy. 86 (2009) 2088–2095.

[9] M. Arvidsson, P. Haro, M. Morandin, S. Harvey, Chem. Eng. Res. Des. 115 (2016) 182–194.

[10] R. Byggningsbacka, N. Kumar, L.E. Lindfors, J. Catal. 178 (1998) 611–620.

[11] N. Kumar, M.P. Dave, Electr. Power Syst. Res. 37 (1996) 189–201.

[12] N. Lempesis, N. Smatsi, V.G. Mavrantzas, S.E. Pratsinis, J. Phys. Chem. C. 122 (2018) 6217–6229.

[13] E.M. Flanigen, J.M. Bennett, R.W. Grose, J.P. Cohen, R.L. Patton, R.M. Kirchner, J. V Smith, Nature. 271 (1978) 512–516.

[14] E. Galli, G. Vezzalini, S. Quartieri, A. Alberti, M. Franzini, 18 (n.d.) 318–322.

[15] D.H. Olson, G.T. Kokotailo, S.L. Lawton, W.M. Meier, J. Phys. Chem. 85 (1981) 2238–2243.

[16] H. Van Koningsveld, F. Tuinstra, H. Van Bekkum, J.C. Jansen, Acta Crystallogr. Sect. B. 45 (1989) 423–431.

[17] H. Van Koningsveld, Acta Crystallogr. Sect. B. 46 (1990) 731–735.

[18] E.L. Wu, S.L. Lawton, D.H. Olson, A.C. Rohrman, G.T. Kokotallo, Wiley, 1979 (83) 2777-2781

[19] J. Klinowski, T.A. Carpenter, L.F. Gladden, Zeolites. 7 (1987) 73–78.

[20] E.L. Wu, S.L. Lawton, D.H. Olson, A.C. Rohrman, G.T. Kokotallo, J. Phys. Chem. 83 (1979) 2777–2781.

[21] S. Quartieri, R. Arletti, G. Vezzalini, F. Di Renzo, V. Dmitriev, J. Solid State Chem. 191 (2012) 201–212.

[22] G.L. Marra, G. Tozzola, G. Leofanti, M. Padovan, G. Petrini, F. Genoni, B. Venturelli, A. Zecchina, S. Bordiga, G. Ricchiardi, Stud. Surf. Sci. Catal. 84 (1994) 559–566.

[23] D.G. Hay, H. Jaeger, J. Chem. Soc. Chem. Commun. 0 (1984) 1433.

[24] E. de Vos Burchart, H. van Bekkum, B. van de Graaf, Zeolites. 13 (1993) 212–215.

[25] J. Haines, O. Cambon, C. Levelut, M. Santoro, F. Gorelli, G. Garbarino, J. Am. Chem. Soc. 132 (2010) 8860–8861.

[26] A. Sartbaeva, J. Haines, O. Cambon, M. Santoro, F. Gorelli, C. Levelut, G. Garbarino, S.A. Wells,

Phys. Rev. B. 85 (2012) 064109.
[27] M. Migliori, E. Catizzone, A. Aloise, G. Bonura, L. Gómez-Hortigüela, L. Frusteri, C. Cannilla, F. Frusteri, G. Giordano, J. Ind. Eng. Chem. 68 (2018) 196–208.
[28] P. Lanzafame, G. Papanikolaou, S. Perathoner, G. Centi, M. Migliori, E. Catizzone, A. Aloise, G. Giordano, Catal. Sci. Technol. 8 (2018) 1304–1313.
[29] P. Lanzafame, K. Barbera, G. Papanikolaou, S. Perathoner, G. Centi, M. Migliori, E. Catizzone, G. Giordano, Catal. Today. 304 (2018) 97–102.
[30] M. Migliori, A. Aloise, E. Catizzone, G. Giordano, Ind. Eng. Chem. Res. 53 (2014) 14885–14891.
[31] D.T. Hayhurst, A. Nastro, R. Aiello, F. Crea, G. Giordano, Zeolites. 8 (1988) 416–422.
[32] H.K. Mao, J. Xu, P.M. Bell, J. Geophys. Res. 91 (1986) 4673.
[33] A.P. Hammersley, S.O. Svensson, M. Hanfland, A.N. Fitch, D. Hausermann, High Press. Res. 14 (1996) 235–248.
[34] B.H. Toby, J. Appl. Cryst. 34 (2001) 210-213.
[35] A.C. Larson and R.B. Von Dreele, Los Alamos National Laboratory Report LAUR 86-748 (2000).
[36] P. Thompson, D.E. Cox, J.B. Hastings, J. Appl. Crystallogr. 20 (1987) 79–83.
[37] H. van Koningsveld, J.C. Jansen, H. van Bekkum, Zeolites. 10 (1990) 235–242.
[38] J.C. Taylor, S.A. Miller, D.M. Bibby, Zeitschrift Für Krist. - Cryst. Mater. 176 (1986) 183–192.
[39] Agilent Technologies, CrysAlisPro (Version 1.171.33.36d), CrysAlisPro (Version 1.171.33.36d), Agil. Technol. Ltd, UK. (2011).
[40] M. Merlini, Marco; Hanfland, High Press. Res. 33 (2013) 511–522.
[41] S.G. Fegan, B.M. Lowe, J. Chem. Soc. Faraday Trans. 1 Phys. Chem. Condens. Phases. 82 (1986) 785.
[42] Y. Matsumura, K. Hashimoto, S. Yoshida, J. Catal. 122 (1990) 352–361.
[43] A. Özgür Yazaydın, R.W. Thompson, Microporous Mesoporous Mater. 123 (2009) 169–176.
[44] S. Quartieri, G. Montagna, R. Arletti, G. Vezzalini, J. Solid State Chem. 184 (2011) 1505–1516.
[45] F. Birch, Finite elastic strain of cubic crystals, Phys. Rev. 71 (1947) 809–824.
[46] R.J. Angel, J. Gonzalez-Platas, M. Alvaro, Zeitschrift Fur Krist. 229 (2014) 405–419.
[47] R. Arletti, G. Vezzalini, A. Morsli, F. Di Renzo, V. Dmitriev, S. Quartieri, J. Solid State Chem. 184 (2011) 1505–1516.
[48] G.D. Gatta, Y. Lee, Mineral. Mag. 78 (2014) 267–291.
[49] G.D. Gatta, P. Lotti, G. Tabacchi, Phys. Chem. Miner. 45 (2018) 115–138.
[50] R. Aiello, J.B. Nagy, G. Giordano, A. Katovic, F. Testa, Comptes Rendus Chim. 8 (2005) 321–329.
[51] D. Comboni, G.D. Gatta, P. Lotti, M. Merlini, M. Hanfland, Microporous Mesoporous Mater. 263 (2018) 86–95.
[52] P. Lotti, G.D. Gatta, D. Comboni, M. Merlini, L. Pastero, M. Hanfland, Microporous Mesoporous Mater. 228 (2016) 158–167.
[53] D. Comboni, · G Diego Gatta, P. Lotti, M. Merlini, · Hanns-Peter Liermann, Phys Chem Miner. 44 (2017) 1–20.

[54] P. Lotti, R. Arletti, G.D. Gatta, S. Quartieri, G. Vezzalini, M. Merlini, V. Dmitriev, M. Hanfland, Microporous Mesoporous Mater. 218 (2015) 42–54.

[55] G.D. Gatta, P. Lotti, Am. Mineral. 101 (2016) 253–265.

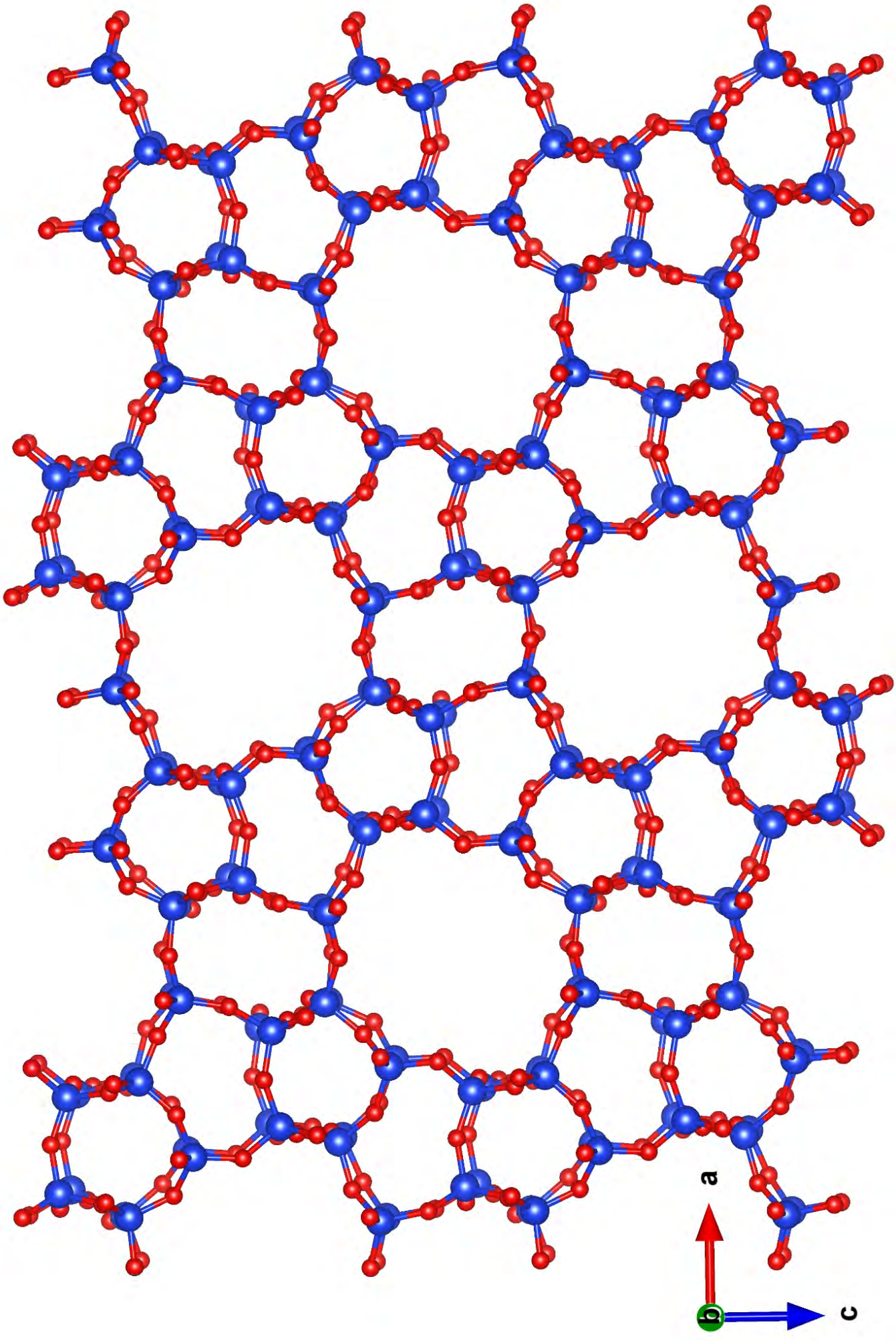
a
c

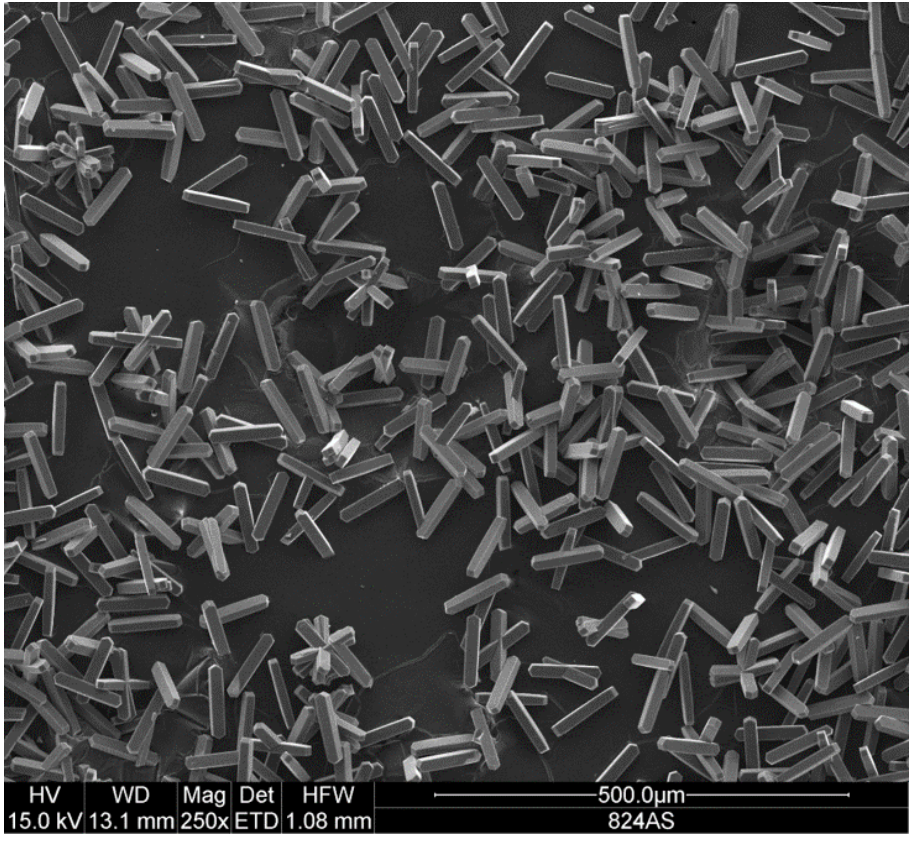
HV
15.0 kV
WD
13.1 mm
Mag
250x
Det
ETD
HFW
1.08 mm
500.0µm
824AS

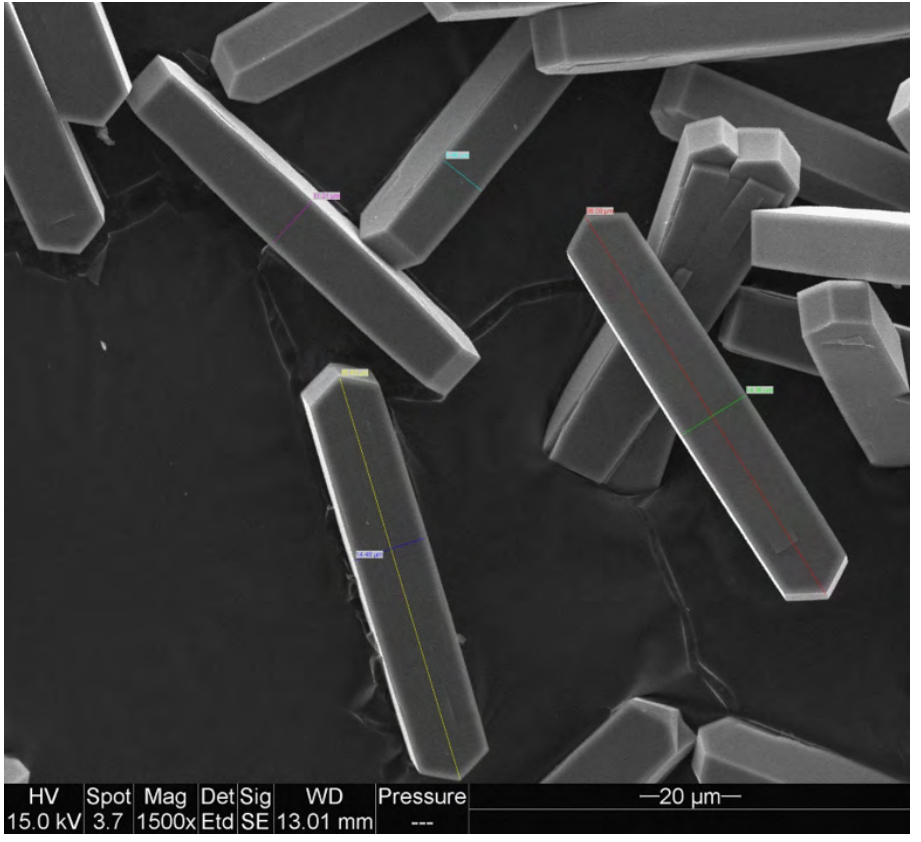
HV
15.0 kV
Spot
3.7
Mag
1500x
Det
Etd
Sig
SE
WD
13.01 mm
Pressure
---
20 µm

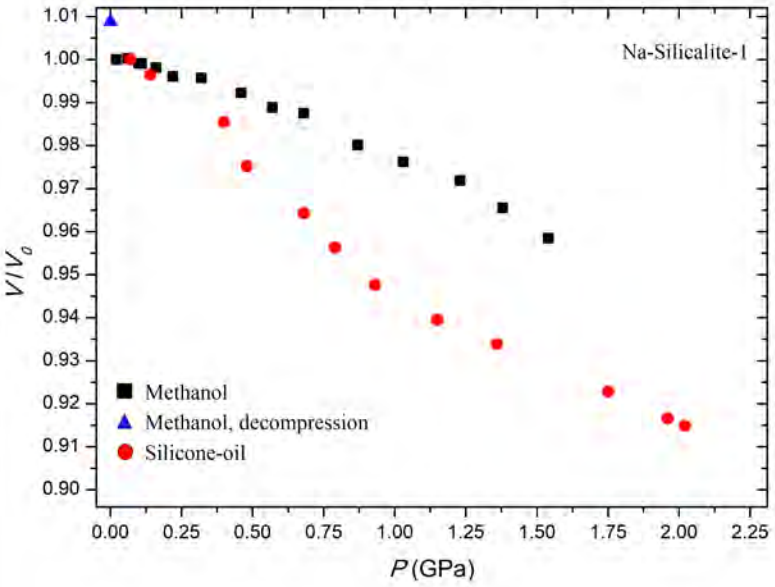
Na-Silicalite-1
Methanol
Methanol, decompression
Silicone-oil
V/V0
P(GPa)

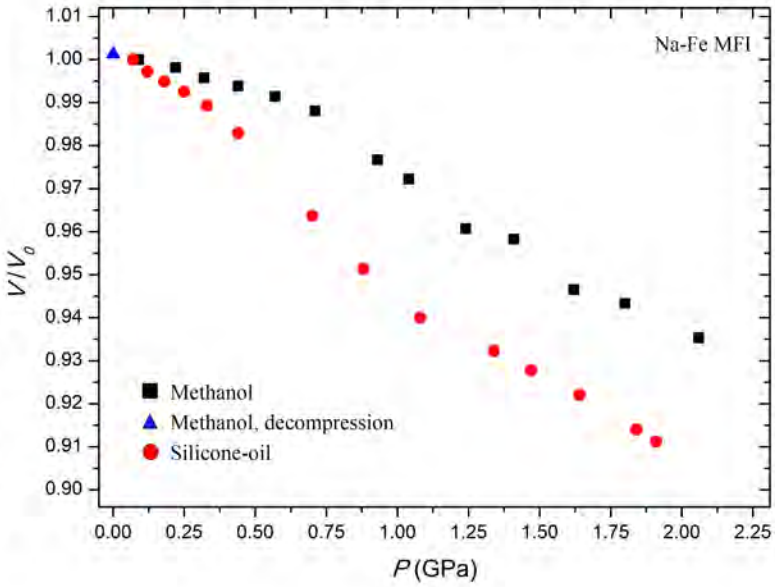
Na-Fe MFI
Methanol
Methanol, decompression
Silicone-oil
V/V0
P(GPa)

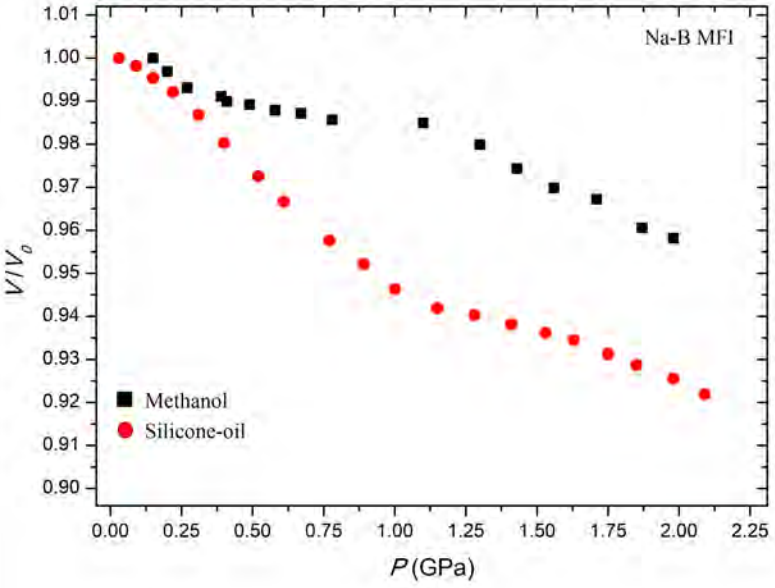
Na-B MFI
Methanol
Silicone-oil
V/V0
P(GPa)

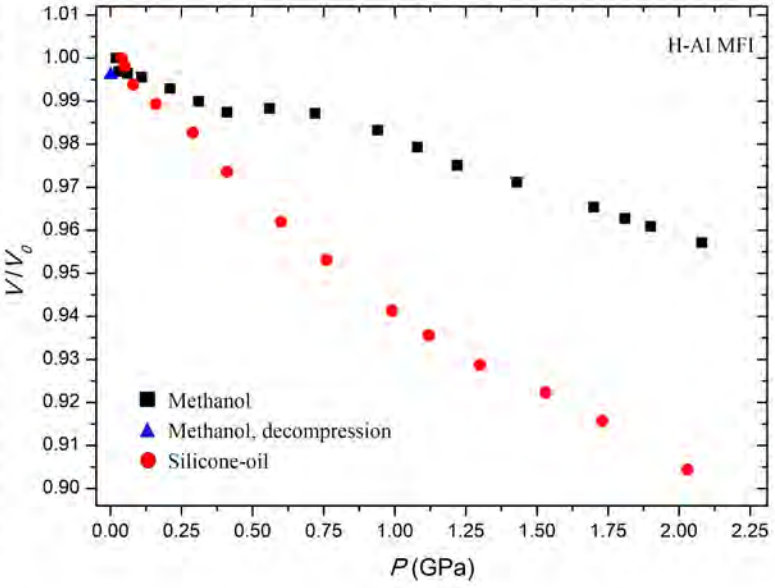
H-Al MFI
Methanol
Methanol, decompression
Silicone-oil
V/V0
P(GPa)

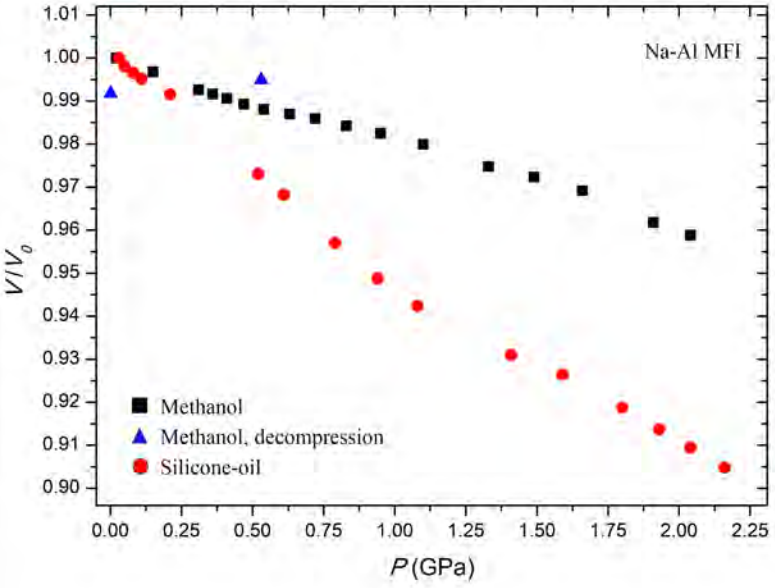
Na-Al MFI
Methanol
Methanol, decompression
Silicone-oil
V/V0
P(GPa)

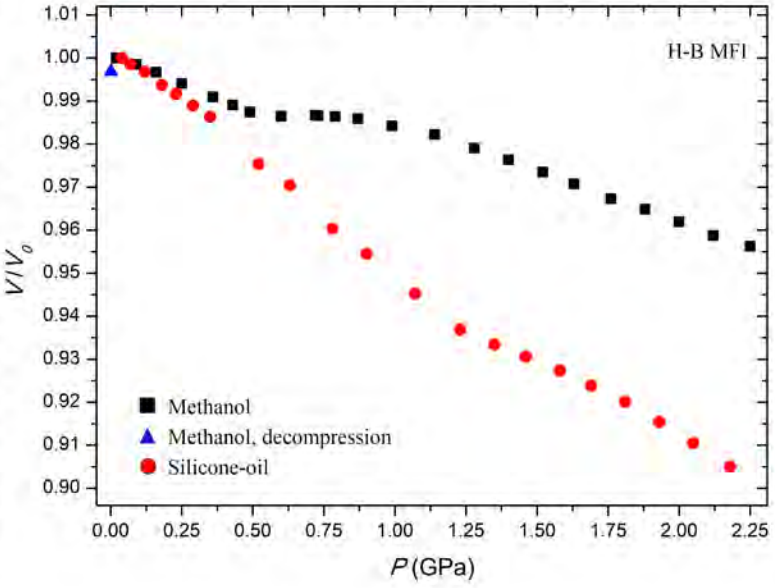
H-B MFI
Methanol
Methanol, decompression
Silicone-oil
V/V0
P(GPa)

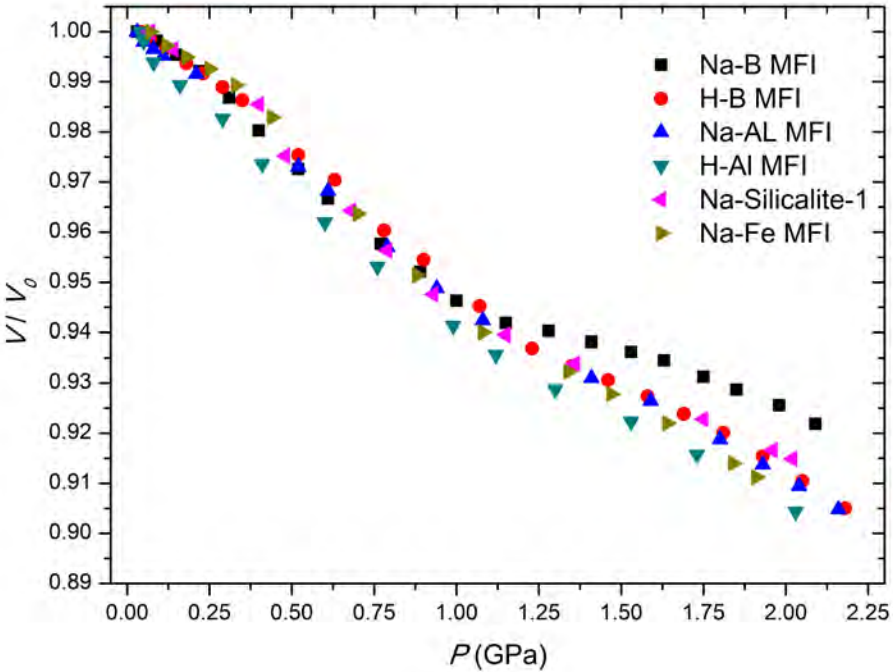
Na-B MFI
H-B MFI
Na-AL MFI
H-Al MFI
Na-Silicalite-1
Na-Fe MFI
V/ V0
P (GPa)

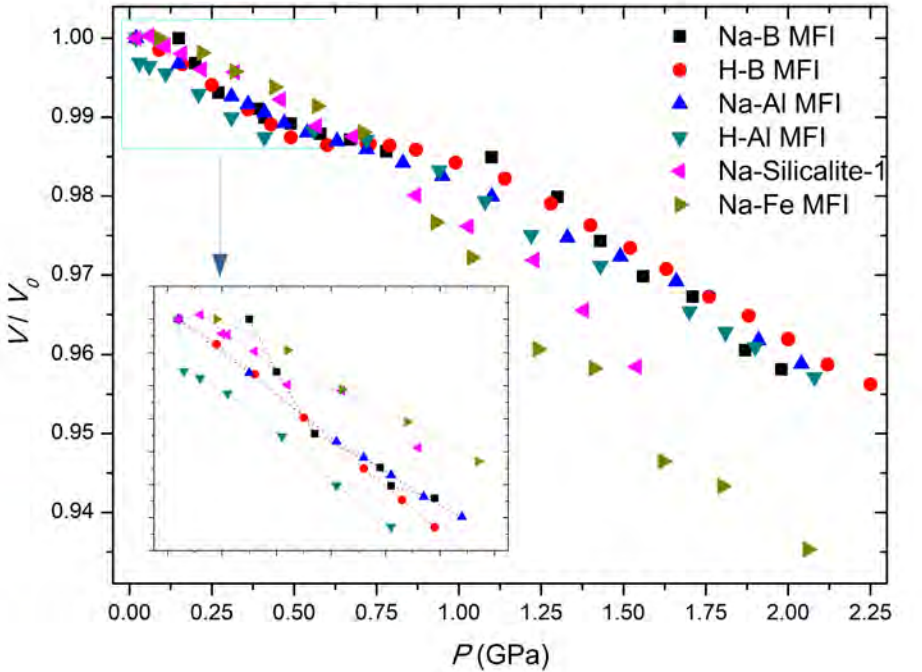
Na-B MFI
H-B MFI
Na-Al MFI
H-Al MFI
Na-Silicalite-1
Na-Fe MFI
V/ V0
P (GPa)

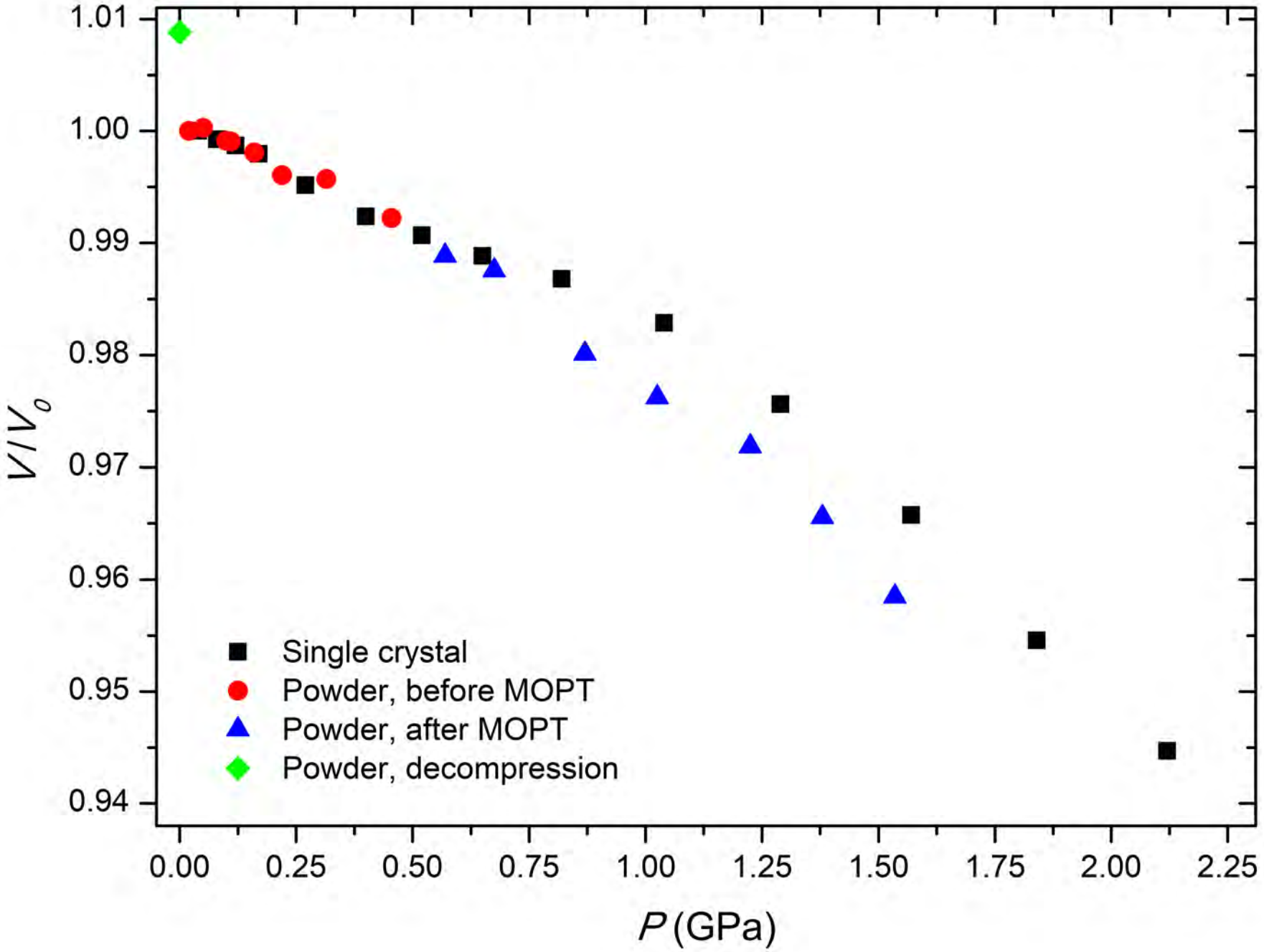
1.01
1.00
0.99
0.98
0.97
0.96
0.95
0.94
V / V0
0.00
0.25
0.50
0.75
1.00
1.25
1.50
1.75
2.00
2.25
P (GPa)
Single crystal
Powder, before MOPT
Powder, after MOPT
Powder, decompression

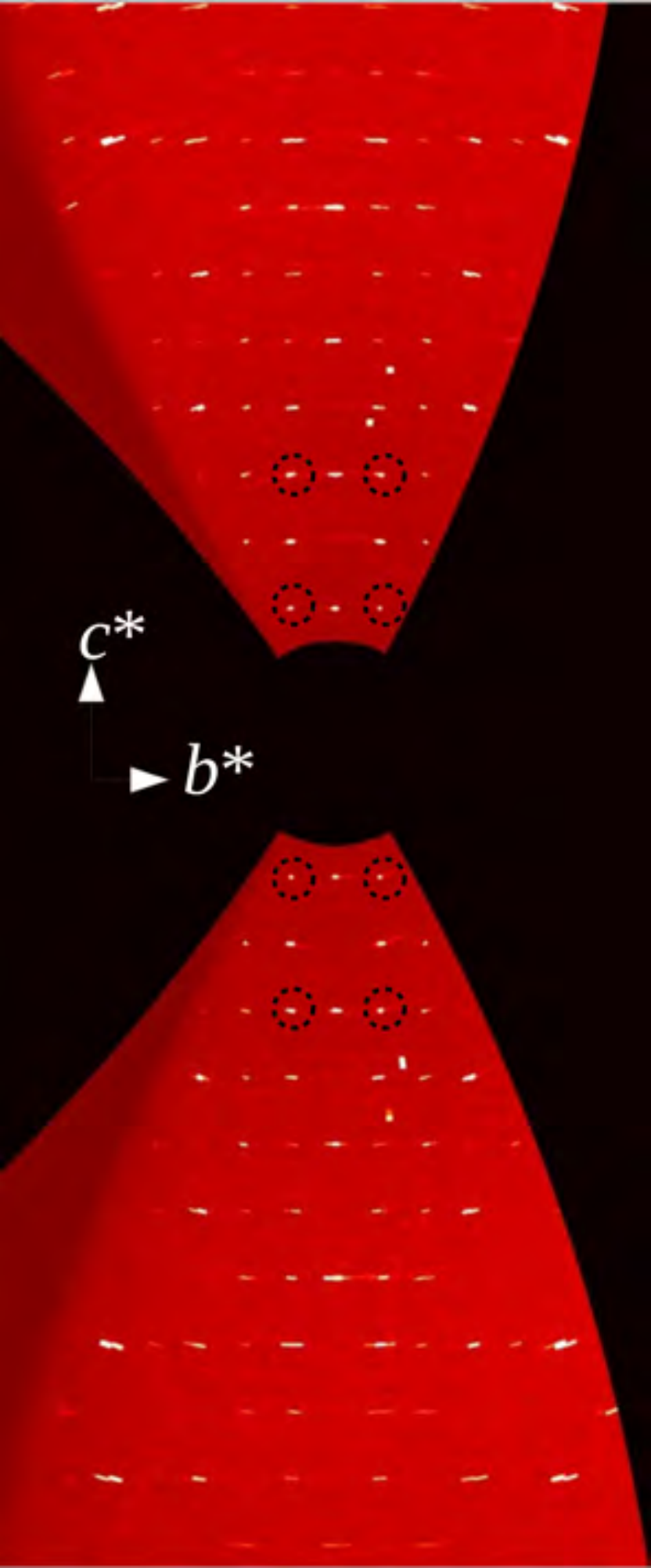
c*
b*

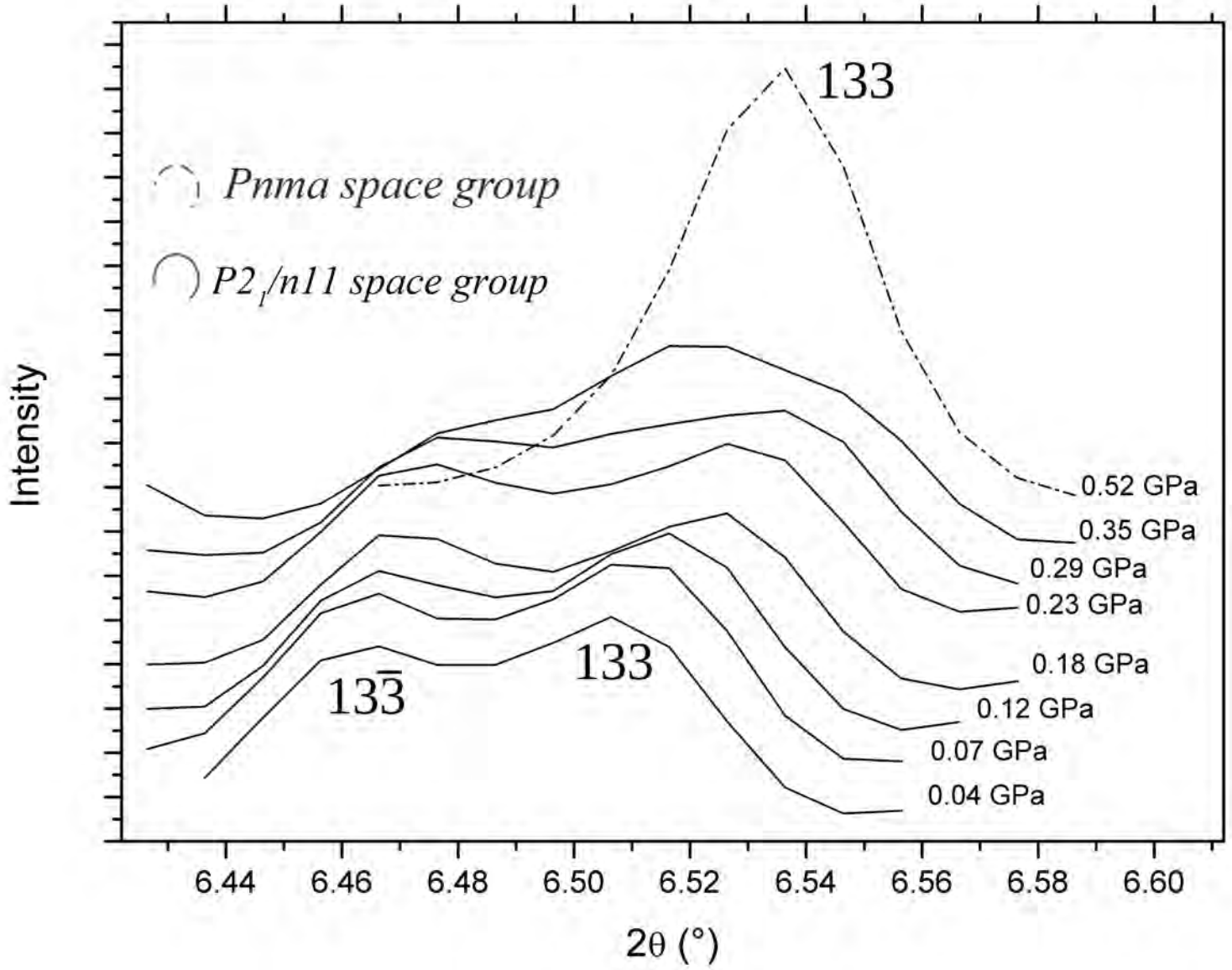
133
Pnma space group
P2₁/n11 space group
0.52 GPa
0.35 GPa
0.29 GPa
0.23 GPa
0.18 GPa
0.12 GPa
0.07 GPa
0.04 GPa
133
13$\bar{3}$
Intensity
6.44
6.46
6.48
6.50
6.52
6.54
6.56
6.58
6.60
2θ (°)

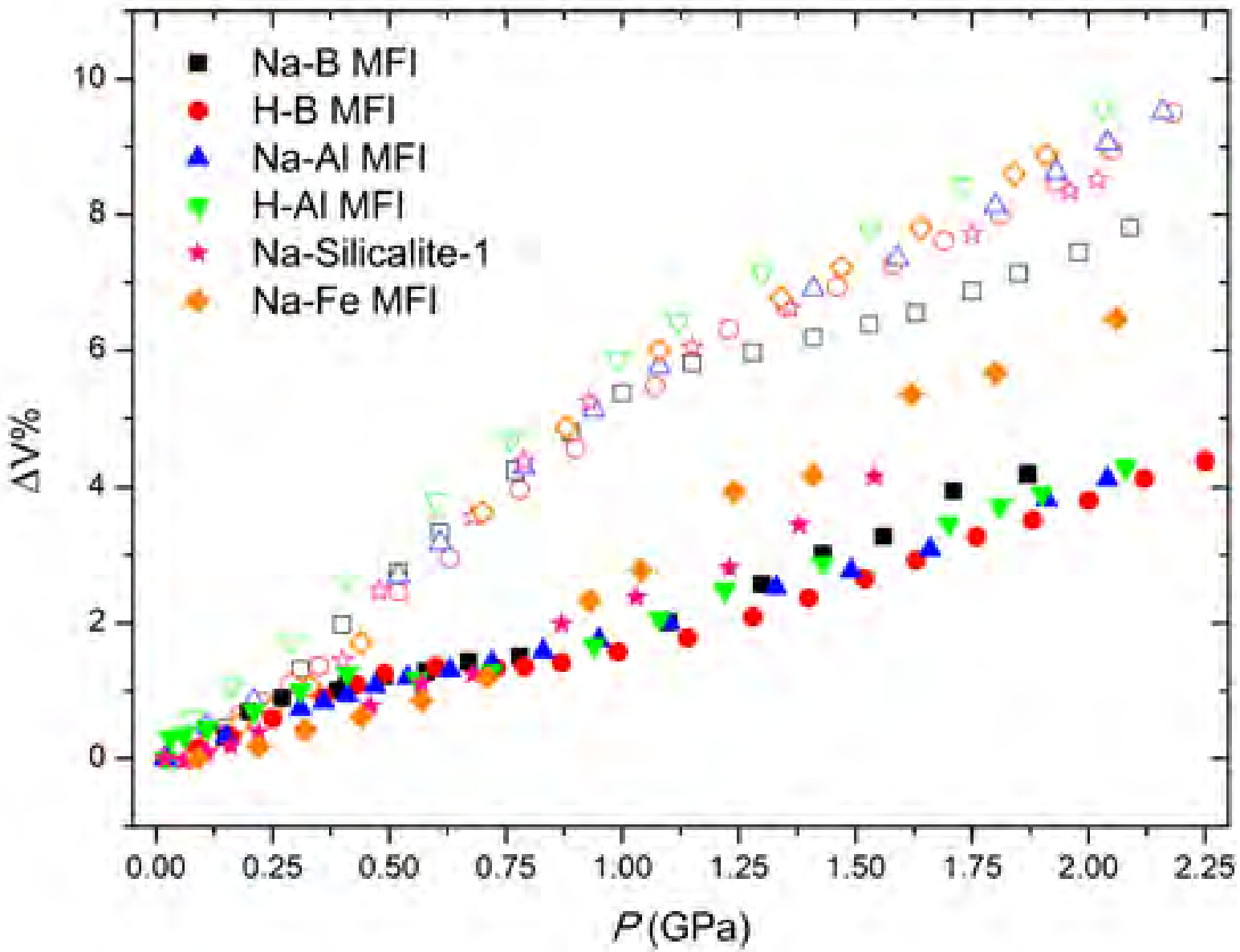
Na-B MFI
H-B MFI
Na-Al MFI
H-Al MFI
Na-Silicalite-1
Na-Fe MFI
ΔV%
0
2
4
6
8
10
0.00
0.25
0.50
0.75
1.00
1.25
1.50
1.75
2.00
2.25
P (GPa)